The $N*$Fisher-Snedecor $\mathcal{F}$ Cascaded Fading Model

Osamah S. Badarneh[1], Sami Muhaidat[2,3], Paschalis C. Sofotasios[2,4], Simon L. Cotton[5],
Khaled Rabie[6], and Daniel B. da Costa[7]

[1]Electrical and Communication Engineering Department, German Jordanian University, Amman 11180, Jordan
(e-mail: osamah.badarneh@gju.edu.jo)
[2]Department of Electrical and Computer Engineering, Khalifa University of Science and Technology,
P. O. Box 127788, Abu Dhabi, UAE   (e-mail: {sami.muhaidat; paschalis.sofotasios}@ku.ac.ae)
[3]Institute for Communication Systems, University of Surrey, GU2 7XH, Guildford, UK
(e-mail: sami.muhaidat@surrey.ac.uk)
[4]Department of Electronics and Communications Engineering, Tampere University of Technology,
FI-33101, Tampere, Finland   (e-mail: paschalis.sofotasios@tut.fi)
[5]Institute of Electronics, Communications and Information Technology, Queen's University Belfast,
BT3 9DT, Belfast, UK (e-mail: simon.cotton@qub.ac.uk)
[6]School of Electrical Engineering, Manchester Metropolitan University, M15 6BH,
Manchester, UK   (e-mail: k.rabie@mmu.ac.uk)
[7]Department of Computer Engineering, Federal University of Ceará, Sobral, CE, Brazil
(e-mail: danielbcosta@ieee.org)

Abstract—The Fisher-Snedecor $\mathcal{F}$ distribution was recently proposed as an accurate and tractable composite fading model in the context of device-to-device communications. The present work derives the product of the Fisher-Snedecor $\mathcal{F}$ composite fading model, which is useful in characterizing fading effects in numerous realistic communication scenarios. To this end, novel analytic expressions are first derived for the probability density function, the cumulative distribution function and the moment of the product of N statistically independent, but not necessarily identically distributed, Fisher-Snedecor $\mathcal{F}$ random variables. Capitalizing on these expressions, we derive tractable closed-form expressions for channel quality estimation of the proposed model as well as the corresponding outage probability and average bit error probability for binary modulations. The offered results are corroborated by extensive Monte-Carlo simulation results, which verify the validity of the derived expressions. It is shown that the number of cascaded channels affects considerably the corresponding performance, as a variation of over an order of magnitude is observed across all signal-to-noise ratio regimes.

I. Introduction

It has been shown extensively that multipath fading and shadowing are two of the most important factors that must be taken into account when characterizing wireless communication channels in both conventional and emerging communications [1]. Based on this, several statistical models have been proposed and utilized for the modeling of multipath fading, such as the Nakagami$-m$, the κ-μ, the η-μ and the α-μ fading distributions [2]–[4]. Similarly, there are different fading distributions that aim to model the shadowing phenomena. The most suitable one is the log-normal distribution, while the gamma distribution is an approximate substitute of log-normal distribution and has bee used extensively owing to its mathematical tractability [1]. Combining the simultaneous effects of multipath fading and shadowing phenomena has led to the formulation and derivation of a range of so-called composite fading distributions, such as the K-distribution, κ-μ shadowed, κ-μ/gamma, η-μ/gamma, and α-μ/gamma, κ-μ/inverse gamma, η-μ/inverse gamma, and extended generalized-K (EGK) distributions [5]–[14]. However, although these composite models are capable of providing adequate characterization of the incurred fading phenomena, quite often their mathematical representation is inconvenient or even intractable. This impacts considerably the formulation of important statistical metrics such as the probability density function (PDF), the cumulative distribution function (CDF), and the moment generating function (MGF), which enable the evaluation of technical performance metrics of interest, such as the symbol error probability, channel capacity, and outage probability (OP). Based on the above, considerable efforts have been made on evaluating the performance of the aforementioned types of multipath fading and composite fading models in different scenarios of interest [15]–[24]. In this context, the authors in [15] introduced a useful general product distribution, known as $N*$Nakagami-m. As in the case of composite fading models, this fading distribution has physical meaning and it arises as a result of the product of N statistically independent, but not necessarily identically distributed (i.n.i.d.), Nakagami-m random variables (RVs). Likewise, Trigui *et al.* introduced the $N*$generalized-K distribution, which is formed as the product of N statistically i.n.i.d. generalized-K RVs [16]. Also, the authors in [17] extended this further, developing the $N*$generalized Nakagami-m (GNM) distribution ($N*$GNM distribution), which represents the product of N statistically

i.n.i.d. GNM RVs. Finally, the authors in [18] introduced the cascaded Weibull, which was generated by the product of i.n.i.d. Weibull RVs.

Capitalizing on the above contributions, numerous investigations have been carried out during the past years in the context of conventional and emerging communication systems. For example, the performance of multihop-intervehicular communication systems with regenerative and non-regenerative relaying over $N*$Rayleigh fading channels was investigated in [19]. Likewise, the authors in [20] analyzed the OP performance of single carrier and multi-carrier systems over $N*$Nakagami-m fading channels under radio frequency impairments. Also, the product of N i.n.i.d. squared generalized-K (KG) RVs is considered in [21], whereas useful statistical metrics of the double-generalized Gamma distribution, were derived in [22] and were used in the analysis of transmit antenna selection systems in vehicle-to-vehicle communications. In the same context, the PDF and CDF of the ratio of two i.n.i.d. α-μ RVs [4] and their applications in spectrum sharing networks were presented in [23]. In [24], the performance of the product of two i.n.i.d. α-μ (so-called α-μ/α-μ) distributions was analyzed, while a relationship between the α-μ/α-μ distribution and the EGK distribution [12] was reported.

It is recalled that a new composite fading distribution, known as the Fisher-Snedecor $\mathcal{F}$ distribution, was recently proposed in [25]. In this composite fading model, the scattered multipath components follow a Nakagami-m distribution, while the root-mean-square (rms) signal is weighted by an inverse Nakagami-m RV. It was shown that this model provides accurate characterization of multipath/shadowing conditions in numerous communication scenarios of interest, such as device-to-device communications. Motivated by this and based on the above, the present work derives the basic statistics of the product of FisherSnedecor $\mathcal{F}$ RVs, it proposes the cascaded Fisher-Snedecor $\mathcal{F}$ fading model and it applies the offered results in the analysis of such systems. Specifically, the contributions of this work are listed below:

- We derive novel closed-form analytical expressions for the PDF, CDF, MGF and moments of the product of Fisher-Snedecor $\mathcal{F}$ variates.
- We employ the derived statistics to analyze the performance of cascaded fading channels.
- We derive the channel quality estimation index (CQEI) for the proposed model and analyze its properties.
- Novel closed-form expressions are deduced for the OP and the average bit error probability for binary modulations.

To the best of our knowledge, these results are currently unprecedented in any literature and given their fundamental nature, they will find use in many areas of mathematical and statistical research. Also, the validity of the offered analytic results is verified through comparisons with respective results from Monte-Carlo simulations.

The reminder of this paper is organized as follows: Section II introduces the necessary preliminary information related to the Fisher-Snedecor $\mathcal{F}$ composite fading model. Then, Section III derives the major statistics of the product of the Fisher-Snedecor $\mathcal{F}$ RVs, while novel theoretical and practical results on the cascaded Fisher-Snedecor $\mathcal{F}$ fading channels are provided in Section IV. Respective numerical results for the considered measures are presented in Section V, while some closing remarks conclude the paper in Section VI.

II. PRELIMINARIES

The received signal in a Fisher-Snedecor $\mathcal{F}$ fading channel is composed of separable clusters of multipath in which the scattered waves have similar delay times, with the delay spreads of different clusters being relatively large. In addition the rms power of the received signal is subject to random variations induced by shadowing. Based on this, the received signal envelope, R, can be represented as

$$R^2 = \sum_{n=1}^{m} A^2 I_n^2 + A^2 Q_n^2 \qquad (1)$$

where m denotes the number of clusters, while I_n and Q_n are independent Gaussian random variables which represent the in-phase and quadrature phase components of the cluster n, with $\mathbb{E}[I_n] = \mathbb{E}[Q_n]$ and $\mathbb{E}[I_n^2] = \mathbb{E}[Q_n^2] = \sigma^2$, and $\mathbb{E}[\cdot]$ denoting statistical expectation. In the above expression A is a normalized inverse Nakagami-m random variable, with $\mathbb{E}[A^2] = 1$, such that

$$f_A(\alpha) = \frac{2(m_s - 1)^{m_s}}{\Gamma(m_s)\alpha^{2m_s+1}} e^{-\frac{m_s-1}{\alpha^2}}. \qquad (2)$$

where m_s represents the scale parameter of the distribution. Based on the above assumptions and following the same methodology as in [25], the new SNR PDF for the Fisher-Snedecor $\mathcal{F}$ fading distribution can be expressed as

$$f_{R_\ell}(r) = \frac{2m_\ell^{m_\ell}((m_{s_\ell} - 1)\Omega_\ell)^{m_{s_\ell}}}{B(m_\ell, m_{s_\ell})}$$
$$\times \frac{r^{2m_\ell-1}}{(m_\ell r^2 + (m_{s_\ell} - 1)\Omega_\ell)^{m_\ell+m_{s_\ell}}}, \quad m_{s_\ell} > 1 \qquad (3)$$

which models multipath fading as a Nakagami-m process and shadowing as an inverse Nakagami-m process. In the above expressions, m_ℓ and m_{s_ℓ} are physical parameters which represent the fading severity and shadowing parameters, respectively, $\Omega_\ell = \mathbb{E}[r^2]$ is the mean power, and $B(\cdot, \cdot)$ is the beta function [26, Eq. (8.384.1)]. The PDF in (3) includes the case of Nakagami-m distribution as $m_{s_\ell} \to \infty$ and its subsequent special cases, such as Rayleigh ($m_\ell = 1$) and one-sided Gaussian ($m_\ell = 1/2$).

During the past years, the Meijer's G-function has been widely used to evaluate several performance metrics of interest in wireless communication systems, such as OP, bit/symbol error probability and channel capacity. The main reason is that it assists in the derivation of tractable analytic expressions, which can be computed straightforwardly since it is a standard built-in function in well-known mathematical software packages such as MAPLE, MATHEMATICA and MATLAB.

It is recalled that the Meijer's G-function represents a complex contour integral with gamma function, namely [27, Eq. (8.2.1.1)]

$$
G_{p,q}^{u,n}\left[z\,\middle|\,\begin{matrix}a_1,a_2,\cdots,a_p\\b_1,b_2,\cdots,b_q\end{matrix}\right]
$$

$$
=\frac{1}{2\pi j}\oint_{\mathcal{L}}\frac{\displaystyle\prod_{i=1}^{u}\Gamma(b_i+s)\prod_{i=1}^{n}\Gamma(1-a_i-s)}{\displaystyle\prod_{i=u+1}^{q}\Gamma(1-b_i-s)\prod_{i=n+1}^{p}\Gamma(a_i+s)}z^{-s}ds,
$$

(4)

where $0\le u\le q$, $0\le n\le p$, a_i and b_i may be complex. The contour $\mathcal{L}$ runs from $c-j\infty$ to $c+j\infty$ such that the poles of $\Gamma(b_i+s), i=1,\cdots,u$, lie to the left of $\mathcal{L}$ and the poles of $\Gamma(1-a_i-s), i=1,\cdots,n$, lie to the right of $\mathcal{L}$. It is also worth highlighting that when $b_i\to\infty$, the Meijer's G-function in (4) can be expressed as [27, Eq. (8.2.2.12)]

$$
\lim_{|b_i|\to\infty}\frac{1}{\Gamma(b_i)}G_{p,q}^{m,n}\left[b_ix\,\middle|\,\begin{matrix}a_1,a_2,\cdots,a_p\\b_i,b_m,\cdots,b_q\end{matrix}\right]
$$
$$
=G_{p,q-1}^{m-1,n}\left[x\,\middle|\,\begin{matrix}a_1,a_2,\cdots,a_p\\b_{i+1},b_m,\cdots,b_q\end{matrix}\right].\quad(5)
$$

III. PRODUCTS OF FISHER-SNEDECOR $\mathcal{F}$ VARIATES

Next, we derive the product of N Fisher-Snedecor $\mathcal{F}$ variates.

Definition 1 (N∗Fisher-Snedecor $\mathcal{F}$ distribution): We define the distribution of the product, X, of N i.n.i.d. Fisher-Snedecor $\mathcal{F}$ RVs R_ℓ, for $1\le\ell\le N$, $R_\ell\sim\mathcal{F}(m_\ell,m_{s_\ell},\Omega_\ell)$, i.e.,

$$
X\triangleq\prod_{\ell=1}^{N}R_\ell.\quad(6)
$$

as $N∗$Fisher-Snedecor $\mathcal{F}$ distributions.

Theorem 1 (Moments): The sth moment of X is given by

$$
\mathbb{E}[X^s]=\prod_{\ell=1}^{N}\frac{\left(\frac{m_\ell}{(m_{s_\ell}-1)\Omega_\ell}\right)^{-\frac{1}{2}s}}{B(m_\ell,m_{s_\ell})}B\left(m_\ell+\frac{1}{2}s,m_{s_\ell}-\frac{1}{2}s\right).
$$

(7)

Proof: The sth order moment of X around the origin can be found using

$$
\mathbb{E}[X^s]=\prod_{\ell=1}^{N}\mathbb{E}[R_\ell^s]=\prod_{\ell=1}^{N}\int_0^\infty r^s f_{R_\ell}(r)dr.\quad(8)
$$

By substituting (3) into (8) and using [26, Eq. (3.194.3)], yields the sth moment of X, which completes the proof. ∎

Lemma 1 (Probability Density Function): The PDF of X is given by (9), at the top of the next page.

Proof: The PDF of X in (6) can be formulated as [28]

$$
f_X(x)=\frac{1}{x}\frac{1}{2\pi j}\oint_{\mathcal{L}}\mathbb{E}[X^s]x^{-s}ds,\quad(10)
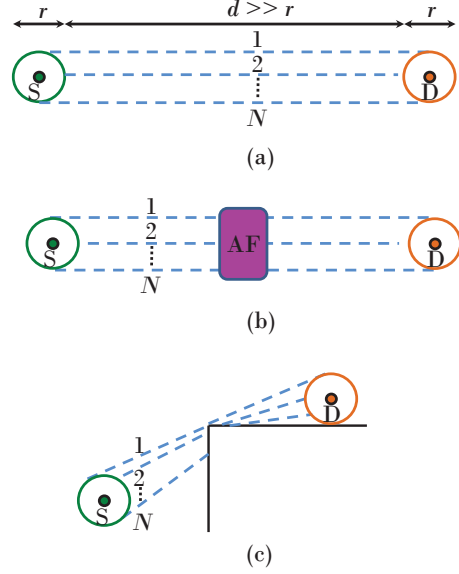$$

Fig. 1: Cascaded fading channels scenarios: (a) Keyhole, (b) amplify-and-forward relay, (c) diffraction.

where $\mathcal{L}$ represents an appropriate contour. To this effect, by inserting (7) into (10), using [26, Eq. (8.384.1)], and carrying out some algebraic manipulations, the PDF of X can be rewritten as

$$
f_X(x)=\frac{1}{\prod_{\ell=1}^{N}\Gamma(m_\ell)\Gamma(m_{s_\ell})}\frac{1}{x}\frac{1}{2\pi j}\oint_{\mathcal{L}}x^{-s}\quad(11)
$$

$$
\times\prod_{\ell=1}^{N}\Gamma(m_\ell+0.5s)\Gamma(m_{s_\ell}-0.5s)\left(\frac{m_\ell}{(m_{s_\ell}-1)\Omega_\ell}\right)^{-\frac{1}{2}s}ds.
$$

(12)

Making the change of variable $t=s/2$ in (11) and using (4) yields the PDF of X, which completes the proof. ∎

It is noted that when $m_{s_\ell}\to\infty$, and using [27, Eq. (8.2.2.14)], along with applying an N-fold limit operation using (5), the PDF in (9) reduces to the PDF of the $N∗$Nakagami-m distribution, as given in [15, Eq. (4)].

Corollary 1 (Cumulative Distribution Function): The CDF of X can be derived as (13), at the top of the next page.

Proof: Using (9) and [27, Eq. (2.24.2.2)] yields the CDF of X. To this effect, when $m_{s_\ell}\to\infty$, eq. (13) reduces to the CDF of $N∗$Nakagami-m distribution in [15, Eq. (7)]. ∎

Corollary 2 (Moment generating function): The MGF of X can be expressed as (14), at the top of the next page.

Proof: The MGF of a RV Z is defined as

$$
M_Z(s)\triangleq\int_0^\infty\exp\left(-s\gamma\right)f_\gamma(\gamma)d\gamma.\quad(15)
$$

Substituting (9) into (15) and then using [27, Eq. (2.24.8.1)], thus equation (14) is obtained. Also, as $m_{s_\ell}\to\infty$, (14) reduces to the MGF of the $N∗$Nakagami-m distribution in [15, Eq. (3)]. ∎

In what follows, the above results are used in the analysis of $N∗$Fisher-Snedecor $\mathcal{F}$ cascaded fading channels.

$$f_X(x) = \frac{2x^{-1} \mathrm{G}_{N,N}^{N,N} \left[x^2 \prod_{\ell=1}^{N} \left(\frac{m_\ell}{(m_{s_\ell}-1)\Omega_\ell} \right) \middle| \begin{matrix} 1-m_{s_1}, 1-m_{s_2}, \cdots, 1-m_{s_N} \\ m_1, m_2, \cdots, m_N \end{matrix} \right]}{\prod_{\ell=1}^{N} \Gamma(m_\ell)\Gamma(m_{s_\ell})}. \tag{9}$$

$$F_X(x) = \frac{\mathrm{G}_{N+1,N+1}^{N,N+1} \left[x^2 \prod_{\ell=1}^{N} \frac{m_\ell}{(m_{s_\ell}-1)\Omega_\ell} \middle| \begin{matrix} 1-m_{s_1}, 1-m_{s_2}, \cdots, 1-m_{s_N}, 1 \\ m_1, m_2, \cdots, m_N, 0 \end{matrix} \right]}{\prod_{\ell=1}^{N} \Gamma(m_\ell)\Gamma(m_{s_\ell})}. \tag{13}$$

$$M_X(x) = \frac{\mathrm{G}_{N+2,N}^{N,N+2} \left[\frac{4}{s^2} \prod_{\ell=1}^{N} \frac{m_\ell}{(m_{s_\ell}-1)\Omega_\ell} \middle| \begin{matrix} \frac{1}{2}, 1, 1-m_{s_1}, 1-m_{s_2}, \cdots, 1-m_{s_N} \\ m_1, m_2, \cdots, m_N \end{matrix} \right]}{\sqrt{\pi} \prod_{\ell=1}^{N} \Gamma(m_\ell)\Gamma(m_{s_\ell})}. \tag{14}$$

IV. CASCADED FADING MODELS

Several realistic wireless transmission scenarios correspond to cascaded fading effects. Some of these cases are illustrated in Fig. 1. As shown in the first scenario, Fig. 1(a), when the source node S and the destination node D are separated by a large distance ($d \gg r$) and are surrounded by many moving and stationary obstacles, the transmitted signal can propagate only through an electromagnetically small aperture, known as a keyhole. The keyhole acts as a source node to the next keyholes, which renders the overall communication channel subject to cascaded fading effects. Likewise, Fig. 1(b) demonstrates the propagation in amplify-and-forward (AF) wireless relay networks, where an AF relay node is essentially a keyhole. As such, the received signal at the relay node will be forwarded to the next relay node until the transmitted signal reaches the destination node. Finally, Fig. 1(c) depicts wireless propagation via diffracting wedges, such as rooftops or street corners. The rooftop or the street corner essentially acts as a multiplier for a large number of statistically independent diffracted rays.

A. Performance of $N*$Fisher-Snedecor Cascaded Channels

Without loss of generality, consider a digital communication system that operates over an $N*$Fisher-Snedecor $\mathcal{F}$ fading channel and in the presence of additive white Gaussian noise (AWGN). In this system, the source node S and the destination node D are located far apart and cannot communicate with each other directly due to constraints such as power constraints and channel fading effects. In this case, the communication can be established through multiple AF-relay nodes, as shown in Fig. 2. The information signal generated by the source node is sent to the next relay node, i.e., R_1. Then, the relay node R_1 forwards it to the next relay node R_2 and this process continues until the information signal reaches the destination node D. To this effect, the instantaneous signal-to-noise ratio (SNR) per symbol at the receiver's antenna is given by:

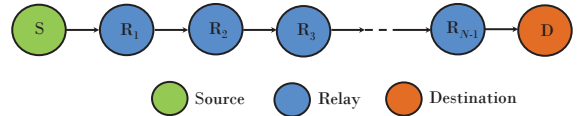$$\gamma = \left(\frac{E_s}{N_0} \right) X^2, \tag{16}$$

Fig. 2: Cascaded fading channels constructed by AF-relay nodes.

where E_s and N_0 represent the average transmitted energy per symbol and the single-sided AWGN, respectively. Based on this, the corresponding average SNR can be expressed as

$$\bar{\gamma} = \left(\frac{E_s}{N_0} \right) \mathbb{E}[X^2] = \left(\frac{E_s}{N_0} \right) \prod_{\ell=1}^{N} \Omega_\ell. \tag{17}$$

Corollary 3 (Probability Density Function): The PDF of the instantaneous SNR γ is given by (18), at the top of the next page.

Proof: After performing a simple transformation of RVs with the aid of (16) and (17), the PDF of γ can be obtained via

$$f_\gamma(\gamma) = \frac{f_X \left(\sqrt{\frac{\gamma}{\bar{\gamma}} \prod_{\ell=1}^{N} \Omega_\ell} \right)}{2\sqrt{\frac{\gamma\bar{\gamma}}{\prod_{\ell=1}^{N} \Omega_\ell}}}, \tag{19}$$

where $f_X(\cdot)$ is defined in (9). This concludes the proof. ∎

Corollary 4 (Cumulative Distribution Function): The CDF of the instantaneous SNR γ can be expressed as (20) at the top of the next page.

Proof: After performing a simple transformation of RVs with the aid of (16) and (17), the CDF of γ can be obtained via

$$F_\gamma(\gamma) = F_X \left(\sqrt{\frac{\gamma}{\bar{\gamma}} \prod_{\ell=1}^{N} \Omega_\ell} \right), \tag{21}$$

where $F_X(\cdot)$ is defined in (13). This completes the proof. ∎

$$f_\gamma(\gamma) = \gamma^{-1} \frac{\mathrm{G}_{N,N}^{N,N}\left[\frac{\gamma}{\bar{\gamma}} \prod_{\ell=1}^{N}\left(\frac{m_\ell}{(m_{s_\ell}-1)}\right) \left|\begin{array}{c} 1-m_{s_1}, 1-m_{s_2}, \cdots, 1-m_{s_N} \\ m_1, m_2, \cdots, m_N \end{array}\right.\right]}{\prod_{\ell=1}^{N}\Gamma(m_\ell)\Gamma(m_{s_\ell})}. \tag{18}$$

$$F_\gamma(\gamma) = \frac{\mathrm{G}_{N+1,N+1}^{N,N+1}\left[\frac{\gamma}{\bar{\gamma}} \prod_{\ell=1}^{N}\left(\frac{m_\ell}{(m_{s_\ell}-1)}\right) \left|\begin{array}{c} 1-m_{s_1}, 1-m_{s_2}, \cdots, 1-m_{s_N}, 1 \\ m_1, m_2, \cdots, m_N, 0 \end{array}\right.\right]}{\prod_{\ell=1}^{N}\Gamma(m_\ell)\Gamma(m_{s_\ell})}. \tag{20}$$

$$M_\gamma(s) = \frac{\mathrm{G}_{N+1,N}^{N,N+1}\left[\frac{1}{\bar{\gamma}s} \prod_{\ell=1}^{N}\left(\frac{m_\ell}{(m_{s_\ell}-1)}\right) \left|\begin{array}{c} 1, 1-m_{s_1}, 1-m_{s_2}, \cdots, 1-m_{s_N} \\ m_1, m_2, \cdots, m_N \end{array}\right.\right]}{\prod_{\ell=1}^{N}\Gamma(m_\ell)\Gamma(m_{s_\ell})}. \tag{22}$$

Corollary 5 (Moments Generating Function): The MGF of the instantaneous SNR γ is given by (22), at the top of the next page.

Proof: Substituting (18) into (15) and then using [27, Eq. (2.24.8.1)], yields (22), which completes the proof. ∎

Corollary 6 (Moments): The k-th moment of the instantaneous SNR γ is given by

$$\mu_k = \mathbb{E}[\gamma^k] = \bar{\gamma}^k \prod_{\ell=1}^{N} \frac{\Gamma(m_\ell+k)\Gamma(m_{s_\ell}-k)}{\Gamma(m_\ell)\Gamma(m_{s_\ell})}\left(\frac{m_{s_\ell}-1}{m_\ell}\right)^k. \tag{23}$$

Proof: The proof follows immediately with the aid of (18) and [27, Eq. (2.24.2.1)]. ∎

B. Channel Quality Estimation Index

The channel quality estimation index (CQEI) is an effective measure that provides insights on the amount of fading of at certain SNR values. It is defined as the ratio of the variance of the instantaneous received SNR γ to the cubed mean of the received SNR γ [29], namely

$$\mathrm{CQEI} = \frac{\mathrm{Var}[\gamma]}{\left(\mathbb{E}[\gamma]\right)^3}. \tag{24}$$

With the help of (23), the CQEI in (24) for the case of $N*$Fisher-Snedecor fading channels is expressed as follows:

$$\mathrm{CQEI} = \frac{1}{\bar{\gamma}}\left\{\prod_{\ell=1}^{N} \frac{\left(1+\frac{1}{m_\ell}\right)\left(1-\frac{1}{m_{s_\ell}}\right)}{\left(1-\frac{2}{m_{s_\ell}}\right)} - 1\right\}. \tag{25}$$

Fig. 3 illustrate the behavior of the CQEI as a function of the average SNR $\bar{\gamma}$. It is observed that the effect of N on the CQEI for fixed values of m and m_s. It is clear that as N increases, the CQEI increases and thus, the system performance degrades.
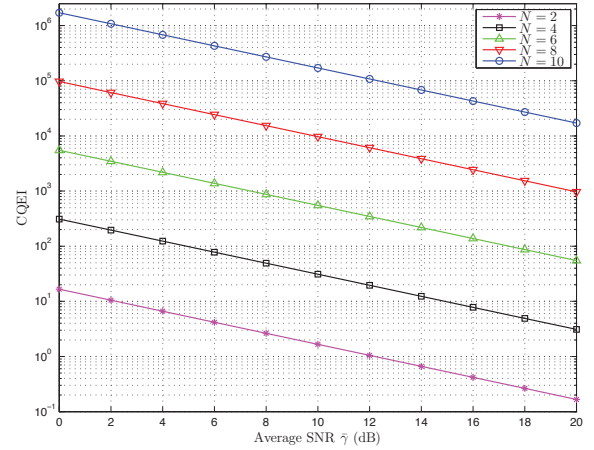

Fig. 3: CQEI versus $\bar{\gamma}$ for i.i.d. $N*$Fisher distributions with $m = 2.5$, $m_s = 2.5$, and $N = 2, 4, 6, 8, 10$.

C. Outage Probability (OP)

The OP is the probability that the instantaneous output SNR γ falls below a certain specified threshold γ_{th}, that is

$$P_{\mathrm{out}} = \mathrm{Pr}[0 \leq \gamma \leq \gamma_{\mathrm{th}}] = \int_0^{\gamma_{\mathrm{th}}} f_\gamma(\gamma)d\gamma = F_\gamma(\gamma_{\mathrm{th}}). \tag{26}$$

It is evident that the OP over $N*$Fisher-Snedecor cascaded fading channels is readily obtained using the corresponding CDF in (20).

D. Average Bit Error Probability (BEP)

The average BEP, $\overline{P}_b$, of a digital communication system is given by

$$\overline{P}_b = \int_0^\infty P_e(\gamma)f_\gamma(\gamma)d\gamma, \tag{27}$$

where $P_e(\gamma)$ denotes the conditional error probability. For the case of binary modulations, $P_e(\gamma)$ is given by

$$P_e(\gamma) = \frac{1}{2\Gamma(b)}\Gamma(b, a\gamma), \tag{28}$$

$$\overline{P}_b = \int_0^\infty \frac{\gamma^{-1}\Gamma(b,a\gamma)\mathrm{G}_{N,N}^{N,N}\left[\frac{\gamma}{\bar\gamma}\prod_{\ell=1}^N\left(\frac{m_\ell}{(m_{s_\ell}-1)}\right)\left|\begin{matrix}1-m_{s_1},1-m_{s_2},\cdots,1-m_{s_N}\\m_1,m_2,\cdots,m_N\end{matrix}\right.\right]}{2\Gamma(b)\prod_{\ell=1}^N\Gamma(m_\ell)\Gamma(m_{s_\ell})}d\gamma. \tag{29}$$

$$\overline{P}_b = \frac{\mathrm{G}_{N+1,N+2}^{N+2,N}\left[\frac{a}{\prod_{\ell=1}^N\left(\frac{m_\ell}{(m_{s_\ell}-1)}\right)}\bar\gamma\left|\begin{matrix}1-m_1,1-m_2,\cdots,1-m_N,1\\m_{s_1},m_{s_2},\cdots,m_{s_N},0,b\end{matrix}\right.\right]}{2\Gamma(b)\prod_{\ell=1}^N\Gamma(m_\ell)\Gamma(m_{s_\ell})}. \tag{30}$$

where $\Gamma(\cdot,\cdot)$ is the complementary incomplete gamma function [26, Eq. (8.350.2)], whereas, a and b are modulation-dependent parameters given in Table I. Hence, by substituting (18) and (28) into (27) yields (29), at the top of the next page. To this effect, the average BEP in (29) can be derived in a closed-form with the aid of [27, Eq. (8.4.16.2)], [27, Eq. (2.24.1.1)], and [27, Eq. (8.2.2.14)], yielding, (30), at the top of the next page.

V. NUMERICAL RESULTS AND DISCUSSIONS

This section presents some illustrative numerical examples for the derived performances metrics of the $N*$Fisher-Snedecor fading model. Also, respective Monte-Carlo simulation results are provided to validate the correctness of the analytic results. To this end, a tight agreement is observed between the analytical and simulated curves in all examined cases.

TABLE I: VALUES OF a AND b IN (28) FOR DIFFERENT BINARY MODULATION SCHEMES.

Constellation	a	b
BPSK	1	$\frac{1}{2}$
DBPSK	1	1
BFSK	$\frac{1}{2}$	$\frac{1}{2}$
NBFSK	$\frac{1}{2}$	1

Fig. 4 illustrates the effect of the number of cascaded channels N on the OP performance for $N = 1,2,3,4$. Also, heavy shadowing conditions are considered i.e., $m_{s_\ell} = 0.5$ with fading severity $m_\ell = 3.5$ and $\gamma_{th} = 0$ dB. For low SNRs values, it is clear that as the number of cascaded fading channel increases, the OP performance improves. On the other hand, at high SNRs values, the OP performance improves when the number of cascaded fading channels decreases. This stems from the inherent characteristics of the keyhole effect and provides interesting insights of realistic communications scenarios.

Likewise, Fig. 5 demonstrates the average bit error probability for $N*$Fisher-Snedecor $\mathcal{F}$ channels with $N = \{2,4\}$ is plotted. As expected, the average bit error probability improves as the number of cascaded channels decreases. For example, a target average BEP of 10^{-3} is achieved at about 13 dB for the case of two cascaded channels and at about
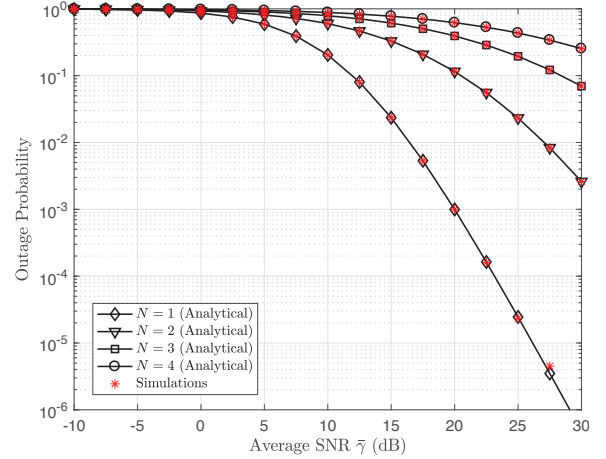

Fig. 4: OP performance as a function of average SNR $\bar\gamma$ for $N = \{1,2,3,4\}$ with heavy shadowing for $m_\ell = 3.5$ and $\gamma_{th} = 0$ dB.
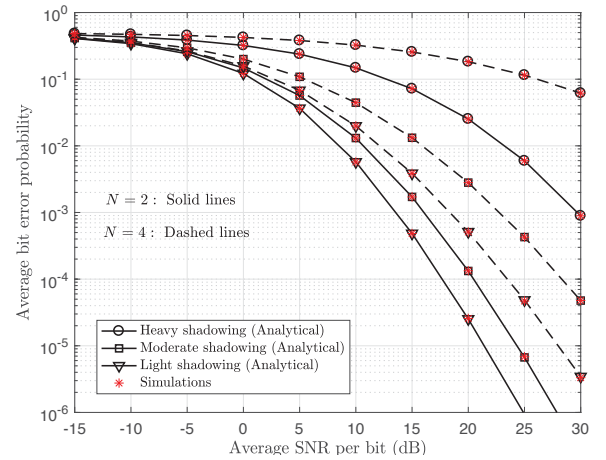

Fig. 5: Average BEP for 4-QAM performance as a function of average SNR per bit for $N = \{2,4\}$ under different shadowing conditions for $m_\ell = 3.5$.

22 dB for the case of four cascaded channels. This shows a considerable variation of nearly 10 dB, which verifies the need for accurate modeling of realistic fading conditions.

VI. Conclusion

The present work derived novel closed-form expressions for the product of N Fisher-Snedecor $\mathcal{F}$ variates which were then extended to the basic statistical measures of the $N*$Fisher-Snedecor $\mathcal{F}$ cascaded fading model. These expressions were then used to derive the channel quality estimation index for the proposed model as well as the outage probability and the average bit-error-probability under such fading conditions. It was shown that the effect of the number of cascaded channels on the system performance is significant since the incurred OP and ABEP variations are at least one order of magnitude. The same also holds for the incurred multipath fading and shadowing conditions as even slight variation of the severity of them has a considerable effect on the system performance across all signal to noise ratio regimes. This verifies the call for accurate characterization and modeling of realistic fading conditions, which will assist largely in the efficient and robust design of future communication systems for versatile and demanding wireless applications of interest.

VII. Acknowledgement

References

[1] M. K. Simon and M.-S. Alouini, *Digital Communications over Fading Channels*. New York: Wiley, 2005.

[2] M. Nakagami, "The m-distribution–A general formula of intensity distribution of rapid fading," in *Statistical Methods in Radio Wave Propagation*, W. Hoffman, Ed. Pergamon, 1960, pp. 3–36.

[3] M. D. Yacoub, "The κ-μ distribution and the η-μ distribution," *IEEE Antennas Propag. Mag.*, vol. 49, no. 1, pp. 68–81, Feb. 2007.

[4] ——, "The α-μ distribution: A physical fading model for the stacy distribution," *IEEE Trans. Veh. Technol.*, vol. 56, no. 1, pp. 27–34, Jan. 2007.

[5] A. Abdi and M. Kaveh, "K distribution: an appropriate substitute for Rayleigh-lognormal distribution in fading-shadowing wireless channels," *Electron. Lett.*, vol. 34, no. 9, pp. 581–582, 1998.

[6] J. F. Paris, "Statistical characterization of κ-μ shadowed fading," *IEEE Trans. Veh. Technol.*, vol. 63, no. 2, pp. 518–526, Feb. 2014.

[7] P. C. Sofotasios and S. Freear, "On the κ-μ/gamma composite distribution: A generalized multipath/shadowing fading model," in *2011 SBMO/IEEE MTT-S International Microwave and Optoelectronics Conference (IMOC 2011)*, Oct. 2011, pp. 390–394.

[8] ——, "The η-μ/gamma composite fading model," in *2010 IEEE International Conference on Wireless Information Technology and Systems*, Aug. 2010, pp. 1–4.

[9] O. S. Badarneh, "Performance evaluation of wireless communication systems over composite α-μ/gamma fading channels," *Wireless Pers. Commun.*, vol. 97, no. 1, pp. 1235–1249, 2017.

[10] S. K. Yoo, S. L. Cotton, P. C. Sofotasios, M. Matthaiou, M. Valkama, and G. K. Karagiannidis, "The κ-μ/inverse gamma fading model," in *2015 IEEE 26th Annual International Symposium on Personal, Indoor, and Mobile Radio Communications (PIMRC)*, Aug. 2015, pp. 425–429.

[11] S. K. Yoo, P. C. Sofotasios, S. L. Cotton, M. Matthaiou, M. Valkama, and G. K. Karagiannidis, "The η-μ/inverse gamma composite fading model," in *2015 IEEE 26th Annual International Symposium on Personal, Indoor, and Mobile Radio Communications (PIMRC)*, Aug. 2015, pp. 166–170.

[12] F. Yilmaz and M. Alouini, "Extended generalized-K (EGK): A new simple and general model for composite fading channels," *CoRR*, vol. abs/1012.2598, 2010. [Online]. Available: http://arxiv.org/abs/1012.2598.

[13] P. C. Sofotasios, S. Freear, "The κ-μ/gamma Composite Fading Model," in IEEE International Conference in Wireless Information Technology and Systems (ICWITS '10), Honolulu, HI, USA, Aug/Sep. 2010.

[14] ——, "The η-μ/gamma and the λ-μ/gamma Multipath/Shadowing Distributions," in Australasian Telecommunication Networks and Applications Conference (ATNAC '11), Melbourne, Australia, Nov. 2011.

[15] G. K. Karagiannidis, N. C. Sagias, and P. T. Mathiopoulos, "$N*$Nakagami: A novel stochastic model for cascaded fading channels," *IEEE Trans. Commun.*, vol. 55, no. 8, pp. 1453–1458, Aug. 2007.

[16] I. Trigui, A. Laourine, S. Affes, and A. Stephenne, "On the performance of cascaded generalized-K fading channels," in *GLOBECOM 2009 - 2009 IEEE Global Telecommunications Conference*, Nov. 2009, pp. 1–5.

[17] F. Yilmaz and M. S. Alouini, "Product of the powers of generalized Nakagami-m variates and performance of cascaded fading channels," in *GLOBECOM 2009 - 2009 IEEE Global Telecommunications Conference*, Nov 2009, pp. 1–8.

[18] N. C. Sagias and G. S. Tombras, "On the cascaded Weibull fading channel model," *Journal of the Franklin Institute*, vol. 344, no. 1, pp. 1 – 11, 2007.

[19] Y. Alghorani, G. Kaddoum, S. Muhaidat, S. Pierre, and N. Al-Dhahir, "On the performance of multihop-intervehicular communications systems over $N*$Rayleigh fading channels," *IEEE Wireless Commun. Lett.*, vol. 5, no. 2, pp. 116–119, Apr. 2016.

[20] A. A. A. Boulogeorgos, P. C. Sofotasios, B. Selim, S. Muhaidat, G. K. Karagiannidis, and M. Valkama, "Effects of RF impairments in communications over cascaded fading channels," *IEEE Trans. Veh. Technol.*, vol. 65, no. 11, pp. 8878–8894, Nov. 2016.

[21] K. Peppas, F. Lazarakis, A. Alexandridis, and K. Dangakis, "Cascaded generalised-K fading channel," *IET Commun.*, vol. 4, no. 1, pp. 116–124, Jan. 2010.

[22] P. S. Bithas, A. G. Kanatas, D. B. da Costa, P. K. Upadhyay, and U. S. Dias, "On the double-generalized Gamma statistics and their application to the performance analysis of V2V communications," *IEEE Trans. Commun.*, vol. 66, no. 1, pp. 448–460, Jan. 2018.

[23] E. J. Leonardo, D. B. da Costa, U. S. Dias, and M. D. Yacoub, "The ratio of independent arbitrary α-μ random variables and its application in the capacity analysis of spectrum sharing systems," *IEEE Commun. Lett.*, vol. 16, no. 11, pp. 1776–1779, Nov. 2012.

[24] O. S. Badarneh, "The α-μ/α-μ composite multipath-shadowing distribution and its connection with the extended generalized-K distribution," *AEU-Int. J. electron. commun.*, vol. 70, no. 9, pp. 1211–1218, 2016.

[25] S. K. Yoo, S. Cotton, P. Sofotasios, M. Matthaiou, M. Valkama, and G. Karagiannidis, "The Fisher-Snedecor $\mathcal{F}$ distribution: A simple and accurate composite fading model," *IEEE Commun. Lett.*, vol. 21, no. 7, pp. 1661–1664, Jul. 2017.

[26] I. S. Gradshteyn and I. M. Ryzhik, *Table of Integrals, Series, and Products*, 7th ed. Academic Press, California, 2007.

[27] A. P. Prudnikov, Y. A. Brychkov, and O. I. Marichev, *Integrals, and Series: More Special Functions*. Gordon & Breach Sci. Publ., New York, 1990, vol. 3.

[28] A. Mathai and R. Saxena, *The H-function with applications in statiistics and other disciplines*. New Delhi: Wiley Eastern, 1978.

[29] A. S. Lioumpas, G. K. Karagiannidis, and A. C. Iossifides, "Channel quality estimation index (CQEI): A long-term performance metric for fading channels and an application in egc receivers," *IEEE Trans. Wireless Commun.*, vol. 6, no. 9, pp. 3315–3323, Sep. 2007.

[30] J. Lu, K. B. Letaief, J. C. I. Chuang, and M. L. Liou, "M-PSK and M-QAM BER computation using signal-space concepts," *IEEE Trans. Commun.*, vol. 47, no. 2, pp. 181–184, Feb. 1999.